Acta Oncologica Vol. 35, No. 7, pp. 809–815, 1996

DNA STRAND BREAKAGE BY ^{125}I-DECAY IN A SYNTHETIC OLIGODEOXYNUCLEOTIDE

Quantitative analysis of fragment distribution

2. PAVEL N. LOBACHEVSKY and ROGER F. MARTIN

The DNA breakage produced by decay of ^{125}I in a double-stranded 41 bp oligodeoxynucleotide was investigated by DNA sequencing gel analysis. Use of both 5′- and 3′-end ^{32}P labelling of the ^{125}I containing strand provided the single-stranded breakage pattern at either side of the ^{125}I-dC. The asymmetric pattern of breakage relative to the ^{125}I-labelled nucleotide enabled deconvolution of two components of breakage. One of them declines very quickly with nucleotide number from ^{125}I-dC and dominates within 4–5 nucleotides. We assume this component to be associated with neutralisation of charged Te atom resulted from decay, or/and with radiation damage to an initial target other than the deoxyribosyl moiety—probably the bases. The second component depends on the geometrical distance between the ^{125}I atom and deoxyribosyl atoms. These two components are responsible for breakage under conditions limiting radical mediated damage, namely in the presence of 2M dimethylsulphoxide. The third component, associated with radical-mediated damage, contributes to the total breakage during incubation in 20mM phosphate buffer alone, and under these incubation conditions dominates the breakage beyond 8–9 nucleotides from ^{125}I-dC. The estimated average numbers of single-stranded breaks produced in the ^{125}I-containing strand by each mechanism in 41-mer oligodeoxynucleotide with ^{125}I-dC at 21st position are respectively 2.33, 0.98 and 0.63.

The main objective of the present study was to determine the sites of DNA single-strand breaks (SSB) arising from decay of single ^{125}I. As described in the preceding paper (1), which presented some of the results for the ^{125}I-dC containing strand with a ^{32}P 5′-end label, the breakage is expressed in terms of probabilities at the various nucleotide sites. In this paper we describe the results for 3′-end labelled counterpart, and use the two sets of data (i.e. 5′ and 3′) to deconvolute the probability function into different components.

An ideal approach to the analysis of DNA breakage by decay of ^{125}I would involve consideration of energy deposited by Auger electrons in a defined target volume. For example an earlier quantitative analysis assumed that the sensitive target was a homogeneous geometric volume occupied by the sugar-phosphate unit, and a total energy deposition of 17.5 eV somewhere in this volume correlated to the critical event for SSB formation (2), and a similar correlation has been reported recently (3). However, in reality the target is chemically quite heterogeneous and individual ionization events within the sensitive target volume may have different outcomes in terms of the probability of SSB formation. Accordingly, we have analyzed the empirical features of single strand breakage, as another approach to gaining insight into potential mechanisms and/or targets associated with the damage. For example

Received 25 August 1995.
Accepted 11 June 1996.
From the Molecular Radiation Biology Laboratory, Trescowthick Research Laboratories, Peter MacCallum Cancer Institute, Melbourne, Australia.
Correspondence to: Dr. Roger F. Martin, Molecular Radiation Biology, Trescowthick Research Laboratories, Peter MacCallum Cancer Institute, Locked Bag 1, A'Beckett Street, Victoria, Australia, 3000. Fax: (613) 9656 1411.
Paper presented at the Third International Symposium on Biophysical Aspects of Auger Processes, August 24–25, 1995, Lund, Sweden.

 ISSN 0284-186X

the use of a molecular modelling package (Biosym 'Insight' and 'Biopolymer') provided the opportunity to consider the probability of breakage in relation to the distance between the ^{125}I atom and potential target structures, as an alternative to the more usual consideration as a function of nucleotide number from the ^{125}I-labelled nucleotide.

Material and Methods

The system and the general experimental procedure used for investigation of ^{125}I decay induced DNA breakage were detailed in the previous paper (1). Some modifications to the general procedure were introduced to construct a double-stranded molecule with ^{32}P 3'-end labelled strand containing ^{125}I-dC.

Unlabelled 20-mer was used to produce a template/primer (41-mer/20-mer) structure for incorporation of ^{125}I-dCTP into this structure by T7 DNA polymerase. The 21-mer oligodeoxynucleotide containing ^{125}I-dC was then purified and annealed with 44-mer template which is 3 nucleotides longer than original template at its 3'-end. This modification enabled the separation, on a denaturing gel, of the top strand after its extension to 41-mer, from the 44-mer template. The 41-mer top strand was then labelled at the 3'-end with α-^{32}P-CoTP by terminal deoxynucleotidyl transferase producing a 42-mer which was then annealed with 41-mer bottom strand. This procedure resulted in a double-stranded molecule with ^{32}P-3'-end labelled strand containing ^{125}I-dC at 22nd position from labelled end. The conditions of incubation and methods of analysis were the same as reported previously (1).

The Biosym modules 'Insight' and 'Biopolymer' were used to build the duplex 41 mer. The sequence is shown in Fig. 1 of the first paper (1). The atomic coordinates generated from 'Insight' were used to find the distance between the iodine atom and each of the deoxyribosyl ring atoms, and the average calculated, for each nucleotide.

Curve fitting analysis was done using nonlinear regression procedure of SigmaPlot 3.0 (Jandel Scientific). This procedure utilizes the Marquardt-Levenberg algorithm to determine the values of parameters. These values and their standard errors are presented as results of curve fitting analysis in the discussion.

Results

The frequencies of registration of 3'-end labelled fragments of length **i** nucleotides, referred as $\mathbf{f_i}$, were calculated as before (1):

$$f_i = N_i/\Sigma N_i (\Sigma f_i = 1), \quad i = 0, 1, \ldots 21, \qquad [1]$$

where N_i is the number of ^{32}P dpm (decay per min) in the individual band of DNA denaturing gel which corresponds to the fragment of length i nucleotides. Eq. [1] is based on the assumption that each decay produces at least one break in the ^{125}I-dC-containing strand between positions 1 and 22. The impact of this assumption on the results is discussed in the previous paper (1) as well as in the following section.

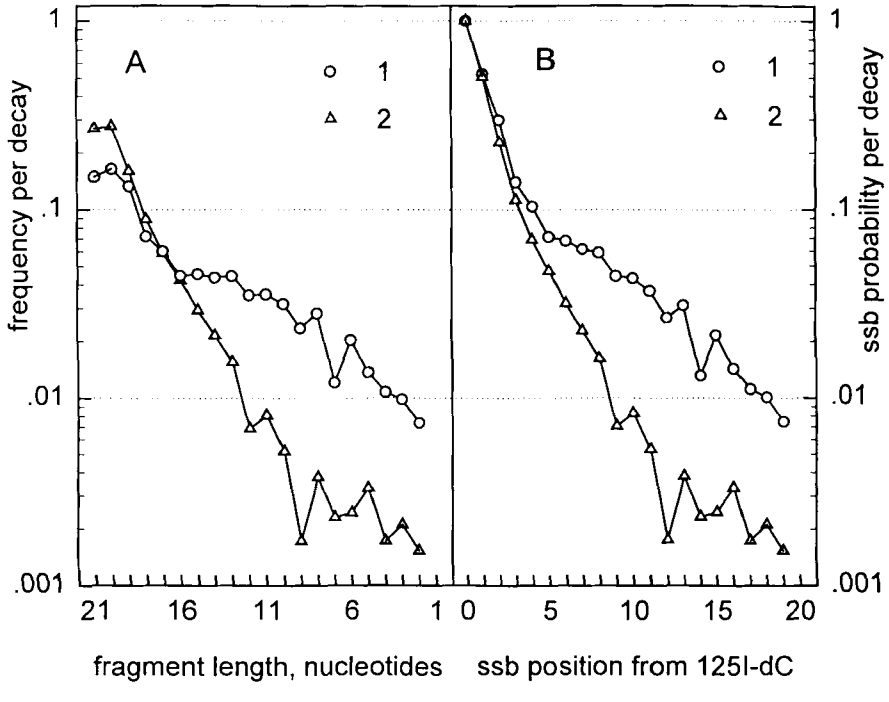

Fig. 1. A) The fragment size distribution and B) probability of SSB at different nucleotide sites relative to the ^{125}I-dC. The 3'-end labelled 42-mer with the ^{125}I-dC at 22nd position was incubated in PB (1) or PB + 2M DMSO (2). The data were obtained from a typical experiment.

Fig. 1A represents the results of a typical experiment: the fragment size distributions for two different conditions of incubation, 20 mM phosphate buffer (PB) and PB + 2M dimethylsulphoxide (DMSO). The fragment size distributions were then converted into the distributions of breakage probability p_i as described previously (1). Fig. 1B represents the distribution of breakage probability.

Discussion

The obvious conclusion from the comparison of results of 5′-end label experiments (Figs. 3 and 5 of the previous paper (1)) with those presented on Fig. 1 is that the general qualitative pattern of breakage is the same on both sides of the ^{125}I-dC, namely, the majority of breakage (around 90%) is within 5–6 nucleotides of the ^{125}I-dC. There is a rapid decrease of breakage probability with increasing distance (nucleotide number) from the ^{125}I-dC, and a considerable protection effect of DMSO at more distant sites (more than 8–9 nucleotides) from the ^{125}I-dC.

Comparison of nucleotide number and distance as correlates of breakage probability. The result of our first attempt to develop a quantitative description of the breakage that would reconcile both 5′- and 3′-end label data (below referred to as 3′-data and 5′-data for brevity) is shown in Fig. 2a. This represents the breakage probabilities as a function of nucleotide number from the ^{125}I-dC in both directions, and clearly shows the asymmetry of the breakage pattern relative to the ^{125}I-labelled nucleotide, compared with the limited scatter within each of the two datasets. The asymmetry is confirmed by the regression analysis, and such a result is not surprising in view of the geometry of the B-DNA helix. Accordingly, we then investigated distances between the ^{125}I atom and each site of cleavage.

There is a considerable evidence that ionization or radical interaction with atoms of sugar-phosphate chain rather than of bases play the dominant role in radiation induced DNA breakage, and the sugar-phosphate component is considered the main target by investigators modelling DNA damage (2–5). We thus determined the distances from the ^{125}I atom to deoxyribosyl atoms using the computer model of our double-stranded molecule, and averaged the distances to each deoxyribosyl unit. Fig. 3 represents these distances for the first 8 nucleotides starting from the ^{125}I-dC for both the 5′ and 3′ directions. The asymmetry of the 5′ and 3′ directions is obvious from this figure. Moreover, comparison of Fig. 2a and Fig. 3 shows that for the first 4 nucleotides from the ^{125}I-dC, the probability of breakage for 3′-data, is lower than for 5′-data corresponding to the greater distances to successive deoxyribosyl units in the 3′ direction, compared with the 5′ direction. Given this qualitative association between this distance and strand breakage, we then investigated the relationship more formally, and the result is shown in Fig. 2b. It is evident that the disagreement between 5′- and 3′-datasets when plotted versus distance between the ^{125}I atom and cleaved deoxyribosyl unit is even more pronounced than in

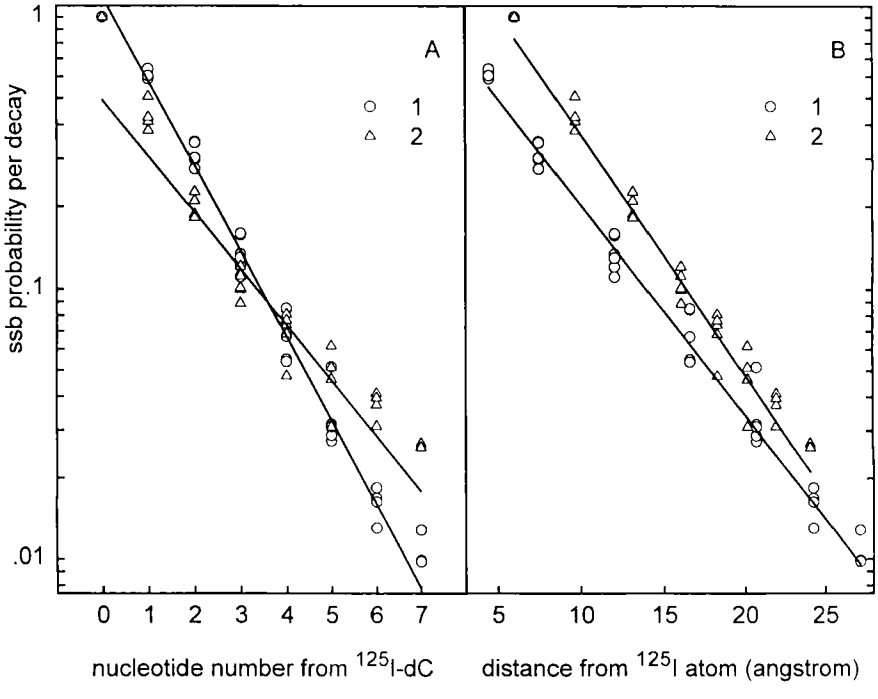

Fig. 2. The probability of SSB within 8 nucleotides represented versus nucleotide number in both directions A) from the ^{125}I-dC and B) as a function of distance between the ^{125}I atom and deoxyribosyl units. **1**—5′- data, 2—3′- data. Five sets of data for each direction are presented. One of the 5′-data sets was obtained from Fig. 5 of the preceding paper (1), and one of the 3′-data sets is included in Fig. 1.

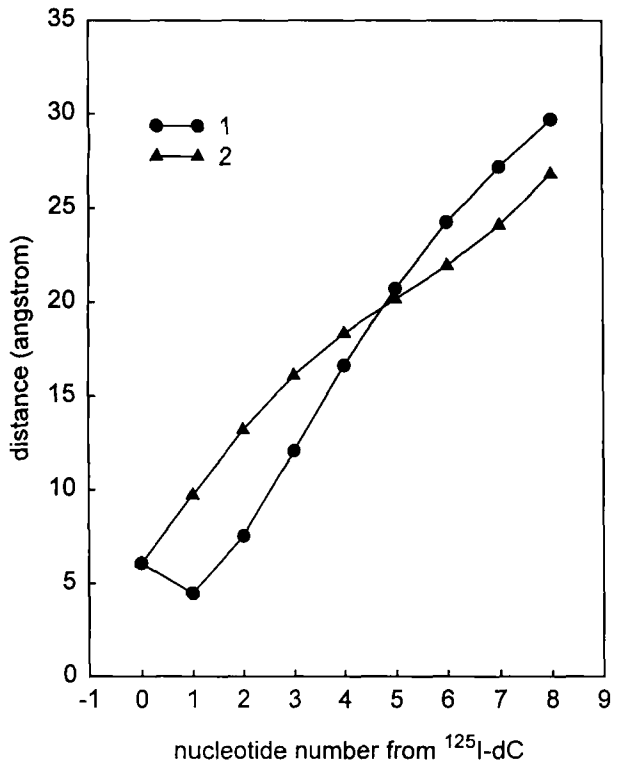

Fig. 3. The distances from the ^{125}I atom to different DNA deoxyribosyl units for the first 8 nucleotides from the ^{125}I-dC. **1**—in 5′-direction, **2**—in 3′-direction. The values are averages of the distances to each of the atoms in deoxyribosyl unit.

the case of the representation versus nucleotide number (see Fig. 2a), and the regression analysis confirms this conclusion. It is worthwhile to note that the disagreement between 5′- and 3′-data decreases with increasing distance and almost disappears beyond 25 A° (nucleotide numbers 7–8), so that geometrical distance may be an appropriate argument for the description of the breakage at longer ranges. Nevertheless, within the range of 7–8 nucleotides the major component of breakage is better described in terms of nucleotide number from the ^{125}I-dC.

Two component analysis. The analysis performed so far shows distinctly that neither nucleotide number nor distance from the ^{125}I atom to deoxyribosyl ring can solely account for the probability of breakage; both factors are involved. This conclusion brought us to the idea that at least two mechanisms, or two targets, contribute to DNA breakage caused by decay of incorporated ^{125}I. The probability of SSB associated with one of these components depends on nucleotide number from the ^{125}I-dC (referred to as the nucleotide number dependent mechanism, NNDM), and the other on geometrical distance from the ^{125}I atom to the deoxyribosyl target (referred to as the distance dependent mechanism, DDM). We determined as well the average distances between the ^{125}I atom and bases (data not shown), and although these data do not exhibit as much asymmetry relative to the ^{125}I atom as distances to deoxyribosyl rings (shown in Fig. 3), the overall requirement for a two-component model remains.

A mathematical approach had to be developed to describe quantitatively the experimental data on the basis of the two-component model. The need for this becomes apparent by considering the fact that if two independent mechanisms can cause SSB at each nucleotide, the overall probability of breakage per decay is not simply the sum of probabilities of breakage by each mechanism and so we assumed that ^{125}I decay produces some events (e.g. ionisations) in the DNA molecule, each of them causing an SSB. We called such events SSB-producing events (SPE) and assigned its number to n_i (**i**–nucleotide number). The number of such events may be more than one at each nucleotide, but at least one SPE is required to produce an SSB at a given site. The number of SPE is an additive value, i.e. if one mechanism produces n_{1i} SPE and another n_{2i} SPE, the total number of SPE is $n_i = n_{1i} + n_{2i}$. Finally, if one assumes a Poisson distribution of SPE at each nucleotide with average n_i, the probability of breakage at position i, p_i as a function of n_i is given by:

$$p_i = 1 - \exp(-n_i). \quad [2]$$

For the NNDM, we found an exponential dependence of the number of SPE on nucleotide number provided the best fit:

$$n_{1i} = n_0 \exp(-i/k), \quad [3]$$

where n_0 and k are parameters, and for the DDM, an inverse square dependence of the number of SPE on distance:

$$n_{2i} = d^2/x_i^2, \quad [4]$$

where x_i is the distance from the ^{125}I atom to the ith nucleotide deoxyribosyl, and d is a parameter.

Curve fitting analysis of the combined 3′- and 5′-datasets (as in Fig. 2) using expressions shown above yielded the following values of parameters:

$$n_0 = 1.49 \pm 0.18$$

$$k = 1.01 \pm 0.06,$$

$$d = 3.08 \pm 0.15 \text{ A}^\circ.$$

Fig. 4 represents the calculated curves and demonstrates the contribution of the each mechanism to the total effect. We should note that Eqs. [3–5] emerged from an empirical curve fitting process in which several functions were compared against the criteria of best fit with minimum number of required parameters, aiming to deconvolute the contribution of each component to the total effect.

Fig. 5 shows the calculated curves for the total effect together with the experimental 3′- and 5′-data for different conditions of incubation. As can be seen, these curves not only give the good description of data, but also predict the

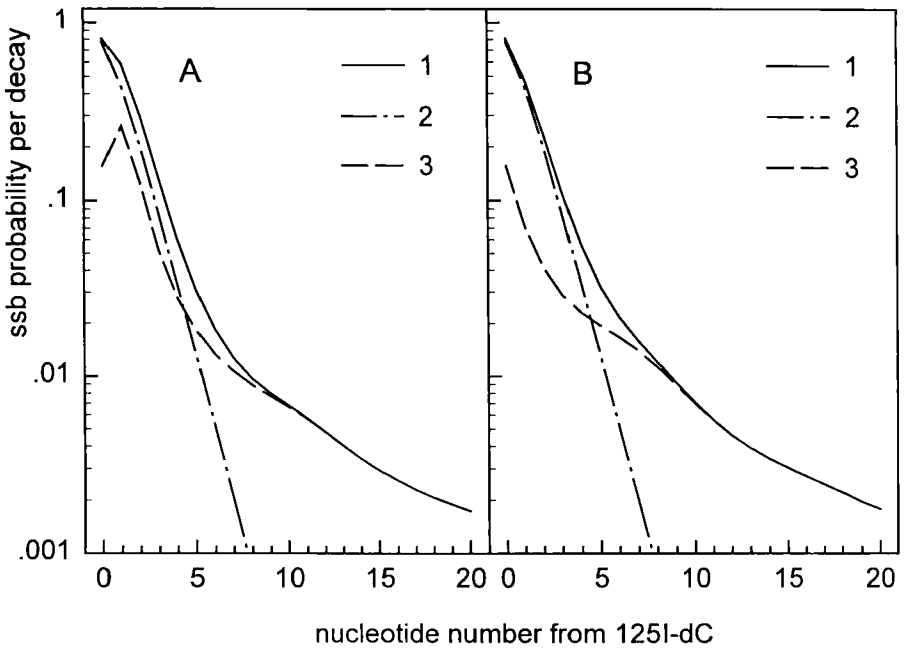

Fig. 4. The contribution of the two components to the total breakage at both sides of the ^{125}I-dC. A—5′-direction, B 3′-direction. **1**—total effect, **2**—the NNDM, **3**—the DDM. The curves are calculated according Eqs [2–4] using values of parameters given in the text.

experimental data for PB + DMSO in the range of nucleotides 8 and more, even though the longer range data were not included in curve fitting analysis. This indicates that two mechanisms are responsible for SSB in PB + DMSO over the whole range of nucleotides.

The NNDM is a dominant within 4–5 nucleotides and contributes equally to breakage at either side of the ^{125}I-dC (curves 2 in Fig. 4). This component declines rapidly with nucleotide number. The contribution of the DDM is different for 5′- and 3′-data (curves 3 in Fig. 4), because of geometrical asymmetry of the sugar-phosphate chain relative to the location of the ^{125}I atom, and this fact determines the asymmetry of the overall breakage pattern. This component provides the absolute majority

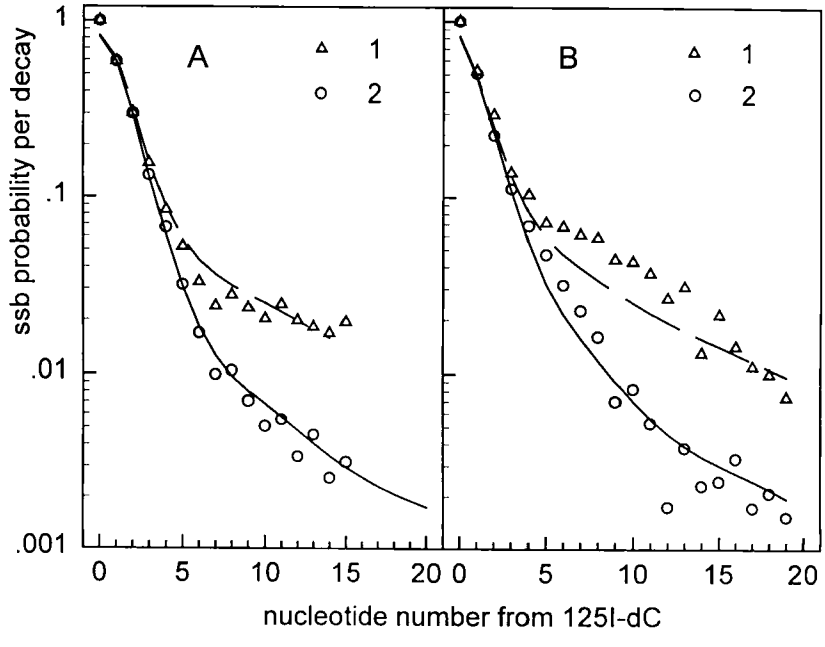

Fig. 5. The calculated curves and experimental data for breakage at both sides of the ^{125}I-dC. A—5′-data, B—3′-data, incubation in PB (1) and PB + DMSO (2). The data were obtained from: A Fig. 5 of previous paper (1), B—Fig. 1 B.

of SSBs beyond 8–9 nucleotides from the ^{125}I-dC in PB + DMSO.

Description of a third, scavengable component. To describe data for PB we assumed a third mechanism which is the radical-mediated and scavengable DNA breakage (referred to as RMM). We assign n_{3i}—the number of SPE produced by this mechanism at each nucleotide—and found an exponential dependence of this value on the distance from the ^{125}I atom satisfied the best fit criteria:

$$n_{3i} = m_0 \exp(-x_i/r), \quad [5]$$

where m_0 and r are parameters.

The curves describing the data for PB on Fig. 5 were calculated on the basis of curve fitting analysis using the values of the n_0, k and d determined on the previous step, and free parameters m_0 and r. The values obtained for these parameters were:

$$m_0 = 0.044 \pm 0.030,$$
$$r = 32.4 \pm 9.8\ A^\circ.$$

Table 1 summarizes the average numbers of SSB produced by each mechanism and in different conditions of incubation. It should be noted that values for PB and PB + DMSO are not the simple sums of values for correspondent mechanisms. As we have mentioned, it is the values of SPE, not the probability of breakage, that are additive values. The overall DMSO protection factor (the ratio of the average SSB numbers) is around 1.2, while in the previous paper we reported 1.1. This apparent discrepancy is due to the smaller contribution of the non-scavengable component (associated with the DDM) to breakage in the 3′-direction of the ^{125}I-dC, and due to the different sizes of the target regions: 21 (5′-half of molecule) in the previous case and 41 (whole molecule) in the present one. One should take into account only half of breakage at the middle nucleotide while estimating the protection factor for half of molecule to avoid distortion of the situation for whole molecule. Thus, we overestimated the breakage at this site by factor 2, thereby increasing the contribution of the non-scavengable mechanism.

The deconvolution of the two components, the NNDM and the DDM, is made on the basis of the asymmetry of the breakage pattern relative to the ^{125}I labelled nucleotide, which in turn is based on the calculation according to Eq. [1] and the inherent assumption that each decay produces at least one break between the ^{32}P-labelled end and the ^{125}I-dC. A calculation aimed at estimating the impact of this assumption showed that normalizing of the 5′ and 3′ fragment size distributions to any value less than 1, with equal probability of breakage at the ^{125}I-dC for both the 5-′ and 3′-datasets, does not affect the asymmetry of breakage pattern significantly in comparison with normalizing to 1.

Mechanistic implications. In naming the components of breakage arising from the deconvolution process, the word 'mechanism' is used in the operational sense, reflecting the basic approach to the analysis. However, it is interesting to consider the significance of each component in terms of possible physico-chemical mechanism of DNA strand breakage. This is indeed the aim of undertaking the experiments.

The nature of the NNDM is the most intriguing, and some possibilities can be suggested. Decay of a ^{125}I atom results in the emission of an average of 21.2 electrons with total per decay energy of 19.8 KeV, and formation of a Te atom which carries a transient positive charge from +8 to +14 (6). The potential energy of this charged atom is around 1 KeV (7). Although this energy contributes only 5% of total delivered energy, it is already contained inside of DNA molecule, while the energy of radiation becomes scattered in the space before being absorbed by DNA molecule again. The energy of the charged atom must be

Table 1a

Three components of ^{125}I-decay induced DNA breakage and their contribution to the total effect

Mechanism	Depends on	Decreased by DMSO	Average number of SSB (from calculated curves)
NNDM	Nucleotide number from ^{125}I-dc	No	2.33
DDM	Distance from ^{125}I atom	No	0.98
RMM	Distance from ^{125}I atom	Yes	0.63

Table 1b

Condition of incubation	Mechanism	Average number of SSB (from experimental data)
PB	NNDM + DDM + RMM	3.67
PB + DMSO	NNDM + DDM	3.02

released by some way, and this process may cause DNA breakage. The neutralization of Te atom has been suggested as a possible mechanism of damage at the ^{125}I-containing nucleotide (7). On the other hand it is possible that the NNDM may involve radiation-induced breakage, but probably with other than deoxyribosyl rings as the target responsible for breakage. Indeed, for these two possible sources or 'instruments' of strand breakage, the nucleotide number dependence of the damage suggests that energy or charge is transmitted and attenuated through the π—electron system of the base pairs in the DNA helix, for which there is experimental evidence (8). This in turn suggests that the bases are an important mediator of SSB. Although the NNDM is rapidly attenuated, it nevertheless contributes the dominant share to the breakage, thus suggesting that energy deposition into bases may be more important than generally assumed.

The nature of the DDM seems more obvious, reflecting ionizing radiation-induced damage to the sugar-phosphate chain. The inverse square dependence on distance is consistent with the geometrical factor of decreasing electron flux, and the non-scavengable property indicates that the damage is mediated by direct ionization. Conversely, the third component is presumably mediated by diffusable radicals.

To conclude, DNA breakage by ^{125}I-decay can be deconvoluted into three components, the first of these describing most of breakage within 4–5 nucleotides of the ^{125}I-dC. The probability of breakage is a function of the number of nucleotides in either direction from the ^{125}I-dC. It is not scavengable. The second component is described by the probability of breakage which is proportional to the inverse square of the distance between the ^{125}I atom and the deoxyribosyl atoms of the target nucleotides. It is not scavengable and dominates beyond 8–9 nucleotides in PB + DMSO conditions. The third component is scavengable and associated with radical-mediated breakage. It dominates in the range more than 8–9 nucleotides in PB conditions.

The identification of the first component, and by inference the important role of the bases as a critical target in mediating strand breakage, is probably the most important outcome of the study. More generally we hope that our results will contribute to the development of more fundamental model of the events leading to strand breakage.

ACKNOWLEDGEMENTS

The project was supported by grant from National Health and Medical Research Council and by the Australia/Russia Cooperation in Medical Science and Public Health.

REFERENCES

1. Kandaiya S, Lobachevsky PN, D'Cunha G, Martin RF. DNA strand breakage by ^{125}I-decay in a synthetic oligodeoxynucleotide: Fragment distribution and evaluation of DMSO protection effect. Acta Oncol 1996; 35: 803–8.
2. Charlton DE, Humm JL. A method of calculating initial DNA strand breakage following the decay of incorporating ^{125}I. Int J Radiat Biol 1988; 53: 353–65.
3. Nikjoo H, Martin RF, Charlton DE, Terrissol M, Kandaiya S, Lobachevsky P. Modelling of Auger-induced DNA damage by incorporated ^{125}I. Acta Oncol 1996; 35: 849–56.
4. Terrissol M. Modelling of radiation damage by ^{125}I on a nucleosome. Int J Radiat Biol 1994; 66: 447–51.
5. Chatterjee A, Magee JL. Theoretical investigation of the production of strand breaks in DNA by water radicals. Radiation Protection Dosimetry 1985; 13: 137–40.
6. Charlton DE, Booz J. A Monte Carlo treatment of the decay of ^{125}I. Radiat Res 1981; 87: 10–23.
7. Charlton DE. The range of high LET effect from ^{125}I decays. Radiat Res 1986; 107: 163–71.
8. Fuciarelli AF, Sisk EC, Miller JH, Zimbrick JD. Radiation-induced electron migration in nucleic acids. Int J Radiat Biol 1994; 66: 505–9.